



Analyst

Biofabrication and Characterization of Multispecies Electroactive Biofilms in Stratified Paper-based Scaffolds

Journal:	<i>Analyst</i>
Manuscript ID	AN-ART-06-2022-001059.R1
Article Type:	Paper
Date Submitted by the Author:	25-Jul-2022
Complete List of Authors:	Elhadad, Anwar; Binghamton University Choi, Seokheun; Binghamton University, Dept of Electrical & Computer Engineering

SCHOLARONE™
Manuscripts

Biofabrication and Characterization of Multispecies Electroactive Biofilms in Stratified Paper-based Scaffolds

Anwar Elhadad¹ and Seokheun Choi^{1,2}*

¹Bioelectronics & Microsystems Laboratory, Department of Electrical & Computer Engineering, State University of New York at Binghamton, Binghamton, New York, 13902, USA

²Center for Research in Advanced Sensing Technologies & Environmental Sustainability, State University of New York at Binghamton, Binghamton, New York, 13902, USA

*Corresponding Author. Email: sechoi@binghamton.edu

Keywords: Electroactive bacteria, electromicrobiology, bacterial consortia, biofilms, paper-based scaffolds, and layer-by-layer construction

Abstract: Bioelectrochemical technologies have attracted significant scientific interest because the effective bacterial electron exchange with external electrodes can provide a sustainable solution that joins environmental remediation and energy recovery. Multispecies electroactive bacterial biofilms are catalysts that will drive the operation of bioelectrochemical devices. Unfortunately, there is a lack of understanding of key mechanisms determining their electron-generating capabilities and syntrophic relations within microbial communities in biofilms. This is because there are no universally standardized models for simple, rapid, reliable, and cost-effective fabrication and characterization of electroactive multispecies biofilms. The heterogeneous and long-term nature of biofilm formation has hampered the development of those models. This work develops novel biofabrication and analysis platforms by creating innovative, paper-based 3-D systems that accurately recapitulate the structure, function, and physiology of living multispecies biofilms. Multiple layers of paper containing bacterial cells were stacked to simulate different layered 3-D biofilm models with defined cellular compositions and

1 microenvironments. Overall bacterial electrogenic capabilities through the biofilm
2 structures were characterized by thoroughly monitoring collective electron flows through
3 different external resistors. Changes in the type of species and order of stacking created
4 biofilm modeling which allowed for the study of their electrogenic performance via
5 variation in electron flow rate output. Furthermore, multi-laminate structures allowed for
6 straightforward de-stacking and layer-by-layer separation for analyses of pH distribution
7 and cellular viability. Our multi-laminate structures provide a new strategy for (i)
8 controlling the biofilm geometry of 3-D bacterial cultures, (ii) monitoring the microbial
9 electrol properties, and (iii) constructing an artificial biofilm layer by layer.

11 **1. Introduction**

12 Extracellular electron transfer (EET) in electroactive bacteria is an extraordinary and
13 transformative process through which self-sustaining and self-maintaining intracellular
14 reactions can be linked to external environments having discontinuous and dependent
15 features [1, 2]. In particular, the study of microbial bidirectional electron exchange with
16 external abiotic electrodes in oxygen-limited environments has evolved into a new,
17 separate field of study, named “electromicrobiology.” The exchange enables sustainable
18 electrochemical synthesis, effective pollutants treatment and remediation, and renewable
19 energy generation in bioelectrochemical systems. Those rapidly developing systems
20 include microbial electrosynthesis (MES), microbial electrolysis cells (MECs), microbial
21 fuel cells (MFCs), and microbial desalination cells (MDCs) [3, 4]. Moreover, as
22 bioelectronics brings unprecedented changes to conventional semiconductor electronics,
23 electroactive bacteria have received increasing attention as an effective interface to bridge
24 the signal gap between biological systems and abiotic electronics [5, 6]. The two most

1
2
3 1 critical requirements to translate these promising EET-based techniques from laboratory
4
5 2 curiosities to practical applications are “performance” that is at least comparable to non-
6
7 3 renewable and abiotic existing techniques and “longevous operation” that can fully and
8
9 4 cost-effectively exploit microbiological self-sustainability. The most practical and feasible
10
11 5 solution can be found by learning from and then emulating natural microbial forms,
12
13 6 behaviors, and processes [7]. Bacteria in natural environments co-exist in densely packed,
14
15 7 spatially structured, multicellular communities defined as biofilms [8]. Individual
16
17 8 microbial species in biofilms enable division of labor, exchange of nutrients and
18
19 9 metabolites between species, and facilitate bacterial survival in and resistance to a hostile
20
21 10 environment through collective group responses [9, 10]. The natural bacterial
22
23 11 multicellular biofilms find the most optimized condition to maximize their viability and
24
25 12 survival by controlling their population and spatial organization [9, 11]. Many previous
26
27 13 studies demonstrated that co-cultured bacterial systems generated longer and better
28
29 14 bioelectrochemical performance in a more self-sustaining manner than monocultures [12-
30
31 15 14]. Furthermore, the bacterial cells embedded in a biofilm enabled a considerably higher
32
33 16 EET rate than planktonic cells because of substantially more compact cell densities and
34
35 17 more available EET pathways in the biofilm [15]. Because of the heterogeneous and long-
36
37 18 term nature of biofilm formation, however, there are no universally used standard biofilm
38
39 19 models, and no studies elucidate adequately multispecies biofilms. Although conceptual
40
41 20 co-culture models with some selected communities have been successfully demonstrated,
42
43 21 the models are limited to conventional 2-D culture platforms that do not reflect the
44
45 22 heterogeneous and complicated 3-D natural environments of multispecies biofilms. When
46
47 23 electroactive biofilms use anaerobic electrode respiration to perform their EET process,
48
49 24 the electron transfer efficiency directly relies on oxygen and electrochemical gradients
50
51
52
53
54
55
56
57
58
59
60

1
2
3 1 formed throughout 3-D biofilms [16, 17]. Depending on microenvironmental changes in
4
5
6
7
8
9
10
11
12
13
14
15
16
17
18
19
20
21
22
23
24
25
26
27
28
29
30
31
32
33
34
35
36
37
38
39
40
41
42
43
44
45
46
47
48
49
50
51
52
53
54
55
56
57
58
59
60

1
2
3
4
5
6
7
8
9
10
11
12
13
14
15
16
17
18
19
20
21
22
23
24
25
26
27
28
29
30
31
32
33
34
35
36
37
38
39
40
41
42
43
44
45
46
47
48
49
50
51
52
53
54
55
56
57
58
59
60

1 the gradients, bacterial metabolic activities vary, further changing the local cell viability

1
2
3 1 and pH, and eventually affecting the performance and longevity of the bacterial systems.
4
5
6
7
8
9
10
11
12
13
14
15
16
17
18
19
20
21
22
23
24
25
26
27
28
29
30
31
32
33
34
35
36
37
38
39
40
41
42
43
44
45
46
47
48
49
50
51
52
53
54
55
56
57
58
59
60

1
2
3
4
5
6
7
8
9
10
11
12
13
14
15
16
17
18
19
20
21
22
23
24
25
26
27
28
29
30
31
32
33
34
35
36
37
38
39
40
41
42
43
44
45
46
47
48
49
50
51
52
53
54
55
56
57
58
59
60

1 Therefore, an in-depth understanding of the key mechanisms underlying the EET process

1
2
3 1 within the biofilm thickness, and of the fundamental factors responsible for determining
4
5
6
7
8
9
10
11
12
13
14
15
16
17
18
19
20
21
22
23
24
25
26
27
28
29
30
31
32
33
34
35
36
37
38
39
40
41
42
43
44
45
46
47
48
49
50
51
52
53
54
55
56
57
58
59
60

1
2
3
4
5
6
7
8
9
10
11
12
13
14
15
16
17
18
19
20
21
22
23
24
25
26
27
28
29
30
31
32
33
34
35
36
37
38
39
40
41
42
43
44
45
46
47
48
49
50
51
52
53
54
55
56
57
58
59
60

1 efficient electron exchange with external electrodes will be critical. Unfortunately, none

1
2
3 1 of the conventional techniques quantify these critical parameters inside biofilms nor
4
5
6
7
8
9
10
11
12
13
14
15
16
17
18
19
20
21
22
23
24
25
26
27
28
29
30
31
32
33
34
35
36
37
38
39
40
41
42
43
44
45
46
47
48
49
50
51
52
53
54
55
56
57
58
59
60

1
2
3
4
5
6
7
8
9
10
11
12
13
14
15
16
17
18
19
20
21
22
23
24
25
26
27
28
29
30
31
32
33
34
35
36
37
38
39
40
41
42
43
44
45
46
47
48
49
50
51
52
53
54
55
56
57
58
59
60

1 control 3-D biofilm formation and thickness. Last but not least, constructing microbial

1
2
3 1 communities having microscale spatial microbial structures remains elusive [12].
4
5
6
7
8
9
10
11
12
13
14
15
16
17
18
19
20
21
22
23
24
25
26
27
28
29
30
31
32
33
34
35
36
37
38
39
40
41
42
43
44
45
46
47
48
49
50
51
52
53
54
55
56
57
58
59
60

1
2
3
4
5
6
7
8
9
10
11
12
13
14
15
16
17
18
19
20
21
22
23
24
25
26
27
28
29
30
31
32
33
34
35
36
37
38
39
40
41
42
43
44
45
46
47
48
49
50
51
52
53
54
55
56
57
58
59
60

1 Conventional lab-based culture models do not form reproducible and controllable

1 multispecies communities with a spatially structured network. What is needed is the
 2 ability to reliably biofabricate 3-D multispecies electroactive biofilm model systems with
 3 a spatial arrangement of community members and to practically characterize key
 4 parameters inside local biofilm and determine critical factors in limiting bacterial EET
 5 efficiency. The model system must mimic *in vivo* environment in biofilms with the ability
 6 to modulate the concentration gradients of the metabolites.

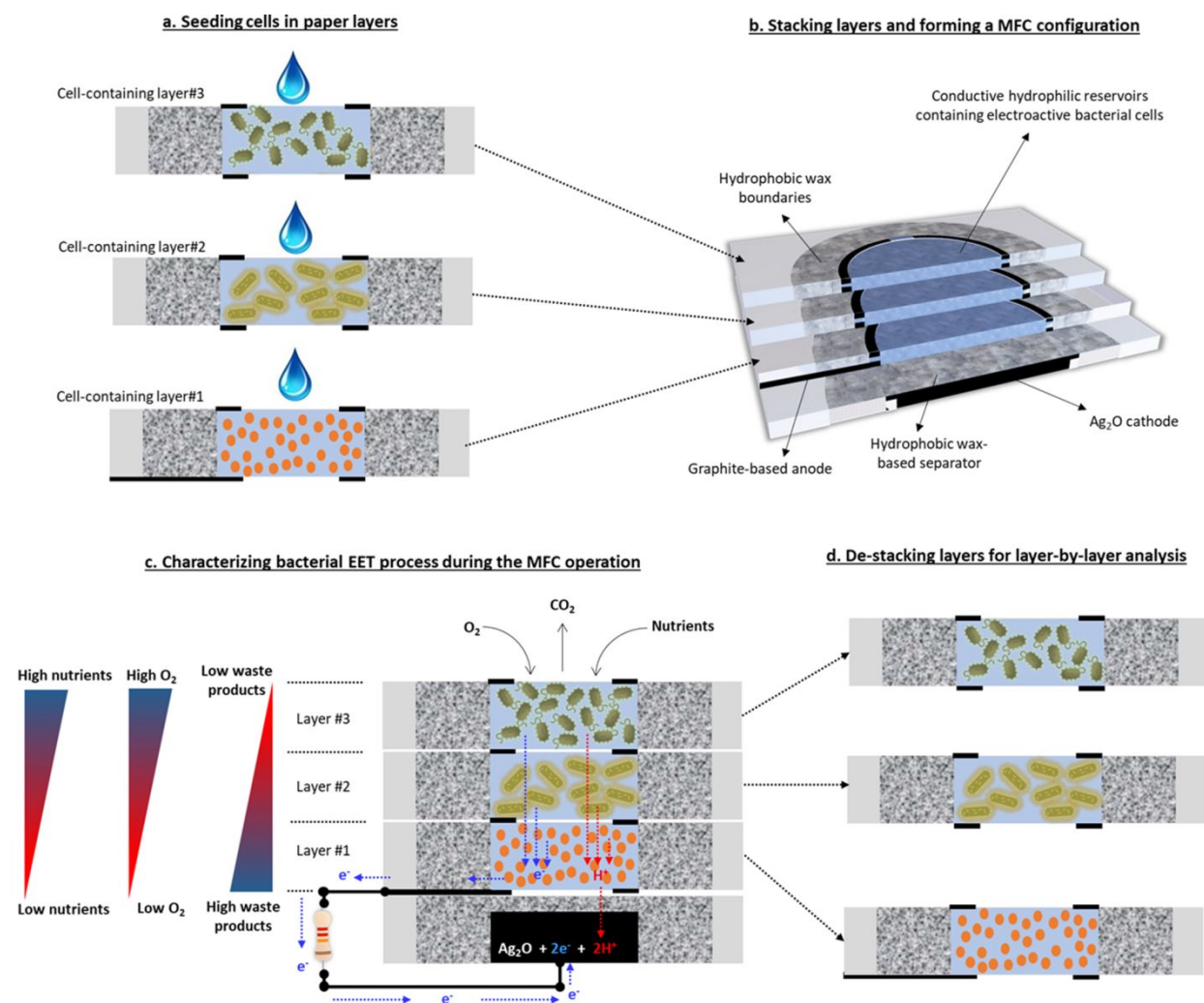


Figure 1. Schematic diagram of our paper-based biofabrication and characterization platform for 3-D multispecies electroactive biofilm models. After individual paper layers are inoculated with electroactive bacteria as scaffolds (a), they are stacked to form a layered 3-D multispecies biofilm model (b). Mass transport of nutrients and oxygen into the 3-D system are regulated to explore the bacterial EET process and current generation within controlled biofilms (c). De-stacking the multi-layered biofilm construct allow layer-by-layer analysis for pH distribution and cellular viability (d).

1
2
3 1 In this work, we create innovative, paper-based biofabrication and characterization
4
5 2 platforms for 3-D multispecies electroactive biofilm engineering (Figure 1). Previously,
6
7 3 paper-based cell culture platforms have been successfully demonstrated for various human
8
9 4 cells [18-20]. However, no studies have explored the biofabrication of stratified biofilm
10
11 5 for better electrochemical performance and to control biofilm functions to optimize the
12
13 6 efficiency of electron transfer. Stacking individual layers of cell-containing paper offers a
14
15 7 modular platform that can mimic 3-D complex biofilm structures with defined cellular
16
17 8 compositions and microenvironments. Multiple layers of paper allow a single species to
18
19 9 form a biofilm with thicknesses determined by the number of layers or a biofilm where
20
21 10 individual species that are confined in separate layers can exchange metabolites.
22
23 11 Individual paper layers can be well patterned by wax printing to define hydrophilic and
24
25 12 hydrophobic regions. The printing is followed by a conductive coating of the non-
26
27 13 conductive hydrophilic areas where bacterial cells are inoculated. Their metabolically
28
29 14 produced electrons can be harvested. By vertically adding another paper layer integrating
30
31 15 a wax-patterned region as a separator and an Ag₂O electrode as a cathode from the bottom
32
33 16 of the bacteria-containing stack, a microbial fuel cell (MFC) can be constructed (Figure 1).
34
35 17 The MFC effectively evaluates the metabolically produced electrons through the bacterial
36
37 18 EET process by allowing a collective measurement of the electron flows as current. The
38
39 19 electrical current values will vary according to different stack configurations and the
40
41 20 number of bacterial layers. The microfibers of paper closely resemble those in
42
43 21 extracellular polymeric substances of the biofilms, providing mechanical integrity and
44
45 22 structural robustness to scaffolds the bacteria use to form biofilms. The porous structure of
46
47 23 paper provides natural gradients of oxygen, nutrients, and bacterial waste products as a
48
49 24 result of diffusional limitations throughout stratified biofilm constructs, consequently
50
51
52
53
54
55
56
57
58
59
60

1 leading to different metabolic activities of bacteria within local biofilms and thus better
2 simulating 3-D in-vivo environments. The biocompatibility and the strong capillary force
3 of paper improve cell adhesion in liquid cultures and stimulate rapid biofilm formation.
4 Finally, multi-laminate biofilm structures allow for straightforward de-stacking and layer-
5 by-layer separation at the end of an MFC operation and provide spatially resolved
6 microbial colonies for further analysis such as pH distribution and cellular viability. This
7 work will revolutionize knowledge about and applications of electromicrobiology by
8 developing novel biofabrication and analysis platforms with a controllable 3-D biofilm
9 model. Those models will help users mimic different biofilm interactions to further study
10 them via de-stacking the 3D paper system. This will support the fundamental study and
11 characterization of microbial EET interactions with electrodes and contribute to an
12 understanding of their EET activities within biofilm thickness and syntrophic relations
13 within microbial communities. Optimizing the spatial arrangement of community
14 members in biofilms and maximizing the metabolic interactions between biofilm layers
15 will be the next-generation strategy for engineering electromicrobiology [12, 13]. The
16 application value of this simulation tool will motivate more innovation in multiple fields
17 of bio-energy conversion, remediation of organic pollutants and toxic metals, and
18 biomedicine.

19
20 **2. Results and discussion**
21 **2.1 Seeding bacterial cells in individual paper layers and stacking the layers for 3-D**
22 **thick biofilm formation.** Bacterial EET-based electrochemical techniques will be able to
23 be realizable when their performance is sufficient for actual applications. Given that the
24 performance depends on the collective EET capabilities of individual cells, it is desirable

1
2
3 1 to design and construct densely packed aggregates of cells [15]. While bacteria can exist
4
5 2 in the form of planktonic cells or biofilms, the cells in biofilm play a more critical role in
6
7 3 the EET process and improve electrochemical performance [21]. The contribution of
8
9 4 planktonic cells represents less than 20% of the total bioelectrochemical performance in a
10
11 5 system [22]. However, electro-microbiological studies have traditionally been limited
12
13 6 because of the lack of models of natural biofilms. Previous static or dynamic biofilm
14
15 7 formation methods with laboratory-scale bioreactors require a relatively long time, skilled
16
17 8 staff, and a considerable amount of reagents, leading to non-reproducible and non-
18
19 9 controllable outputs [23]. Recent microfluidic approaches are limited to small populations
20
21 10 that cannot mimic a thick *in vivo* biofilm environment [24, 25]. Even the latest advances
22
23 11 in 3-D printing require complicated and time-consuming processes for bioink preparation,
24
25 12 and it is controversial whether the 3-D printed biofilm resembles the actual *in vivo* biofilm
26
27 13 environments [26, 27]. Above all, reported work with electrogenic bacterial cells for
28
29 14 electroactive biofilm formation is unavailable or quite limited.

30
31
32
33
34
35 15 Here we propose a 3-D, paper-based biofilm model as a new technique for simple,
36
37 16 rapid, and cost-effective electroactive biofilm fabrication and characterization. A
38
39 17 hydrophilic paper can serve as a scaffold for biofilm formation and multiple layers of
40
41 18 paper containing bacterial cells can be readily stacked to control the biofilm's thickness
42
43 19 (Figures 2 and 3). First, hydrophobic and hydrophilic regions of the individual papers
44
45 20 were well defined by printing and thermally impregnating hydrophobic wax (Figures 2a
46
47 21 and 2b). Then, we coated non-conducting hydrophilic regions with a conducting material,
48
49 22 poly(3,4-ethylenedioxythiophene):polystyrene sulfonate (PEDOT:PSS). The coating
50
51 23 enabled the regions to have open pores and hydrophilic features for subsequent liquid-
52
53 24 based bacterial sample introduction [28]. Because of the excellent biocompatibility,
54
55
56
57
58
59
60

1 bacterial affinity, and electrocatalytic capability of the PEDOT:PSS, bacterial cell
2 adhesion can be significantly improved in the engineered paper (Figure 2c). Circular
3 graphite electrodes were then screen-printed at the periphery of the conductive regions on
4 both sides of the paper to act as the current collector and the conductive interface when
5 being stacked (Figures S1, 2, and 3). When bacterial cells with an optical density at 600
6 nm (OD600) of 1.0 were introduced into the engineered hydrophilic region, the capillary
7 force pulled the cells through the paper layers, resulting in fast accumulation and
8 acclimation of the cells. To ensure reducing the unintended biases caused by the user
9 fabrication process, we made it where every step of the fabrication process is micro-
10 fabricable and every step can be automated.

11

12

1

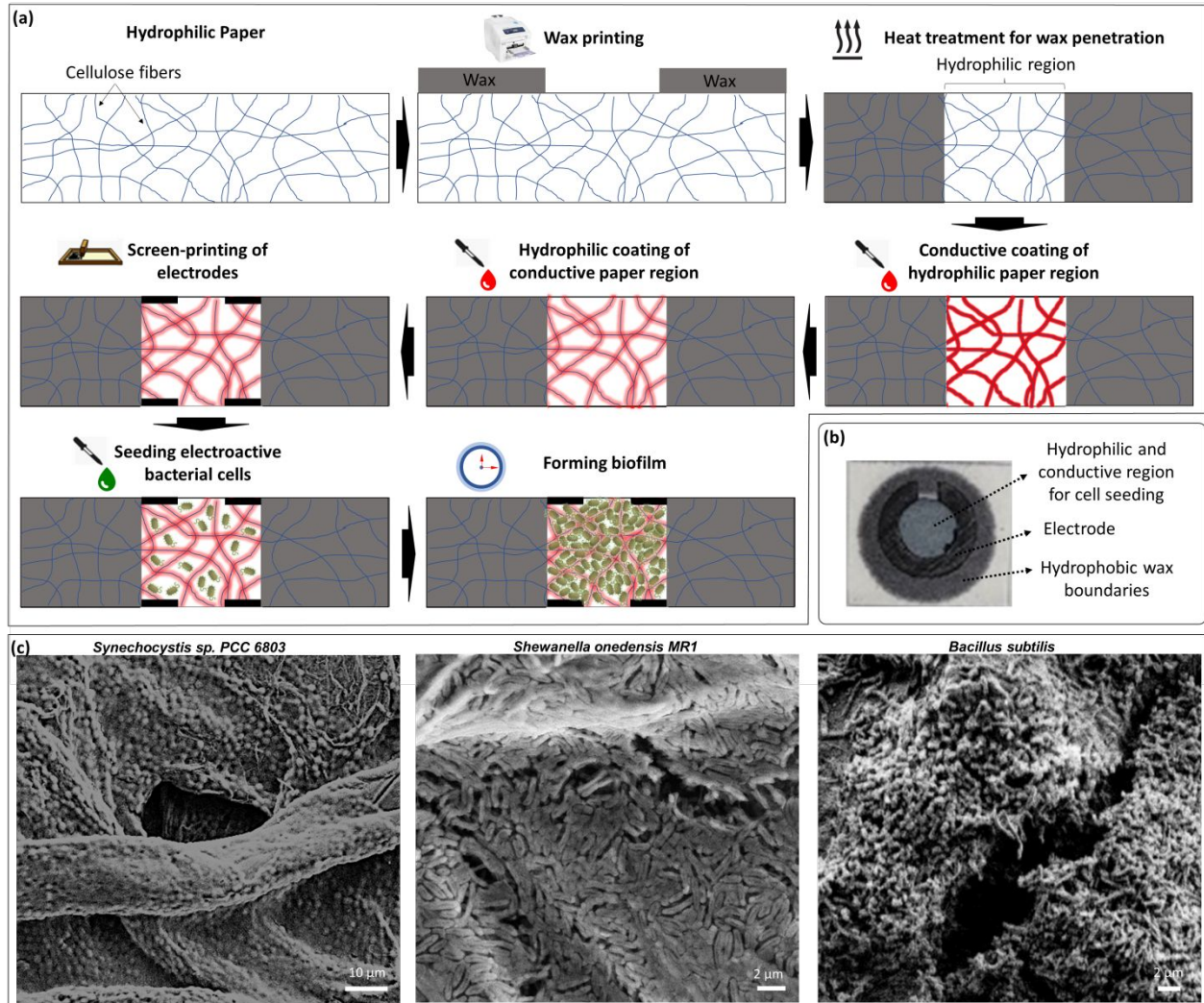


Figure 2. Seeding cells in engineered paper layers. The part of paper is engineered to be conductive and hydrophilic for bacterial cell inoculation and their biofilm formation. To effectively harvest microbial electrons metabolically produced, the non-conductive paper fibers are coated with a conductive PEDOT:PSS polymer. Hydrophilic coating is necessary to improve the capillary force of the treated paper region for rapid wicking of aquatic cell culture and cell adhesion. (a) Process flow for paper engineering and biofilm formation, (b) a picture of the engineered paper, and (c) scanning electron microscope (SEM) images of three individual bacterial biofilms formed in the engineered papers.

2 Rapid biofilm formation can be attributed to (i) paper's porosity throughout its large
 3 surface area and 3-D nature-like bacterial habitat, (ii) the biocompatibility and bio-affinity
 4 of the coated PEDOT:PSS to promote cell adhesion, and (iii) paper's hydrophilicity to
 5 strongly absorb the aquatic bacterial culture. The paper-based biofilm model can
 6 standardize simple and rapid biofilm formation and EET evaluation by allowing easy

1 seeding of bacterial cells with a micropipette. The procedure has potential high-
2 throughput capabilities and allows easy assembly of a thick biofilm by simply stacking the
3 layers. Individual layers were tightly attached by using a spray adhesive and paper clips,
4 resulting in precise control of the thickness of the 3-D biofilm (Figure S1). The spray was
5 only on the unused sides of the paper to hold the structure still to maintain consistency and
6 did not affect any parameters of the experiments conducted. A mask was used to
7 completely prevent any adhesive chemical from getting in contact with the anode,
8 cathode, or separator. Overall bacterial electrogenic EET capabilities through the biofilm
9 thickness were characterized by thoroughly monitoring the collective electron flows
10 through different external resistors (Figure 3). Comprehensive polarization curves and
11 output power densities as a function of current density were well obtained for different
12 bacterial species and their different biofilm thickness (Figure S2). *Synechocystis sp.*
13 *PCC6803*, *Shewanella oneidensis MRI*, and *Bacillus subtilis* were inoculated in BG-11,
14 Luria Broth (LB), and Soy Broth (SB), respectively. Each medium without bacterial cells
15 generated negligible electrical output compared with the cell-containing culture,
16 indicating that all current/power productions originated from bacterial metabolism (Figure
17 S3). Although this system-level analysis does not include cellular or genetic level
18 assessment, it is sufficient to obtain a comprehensive understanding of the electrogenic
19 dynamics of microbial biofilms.

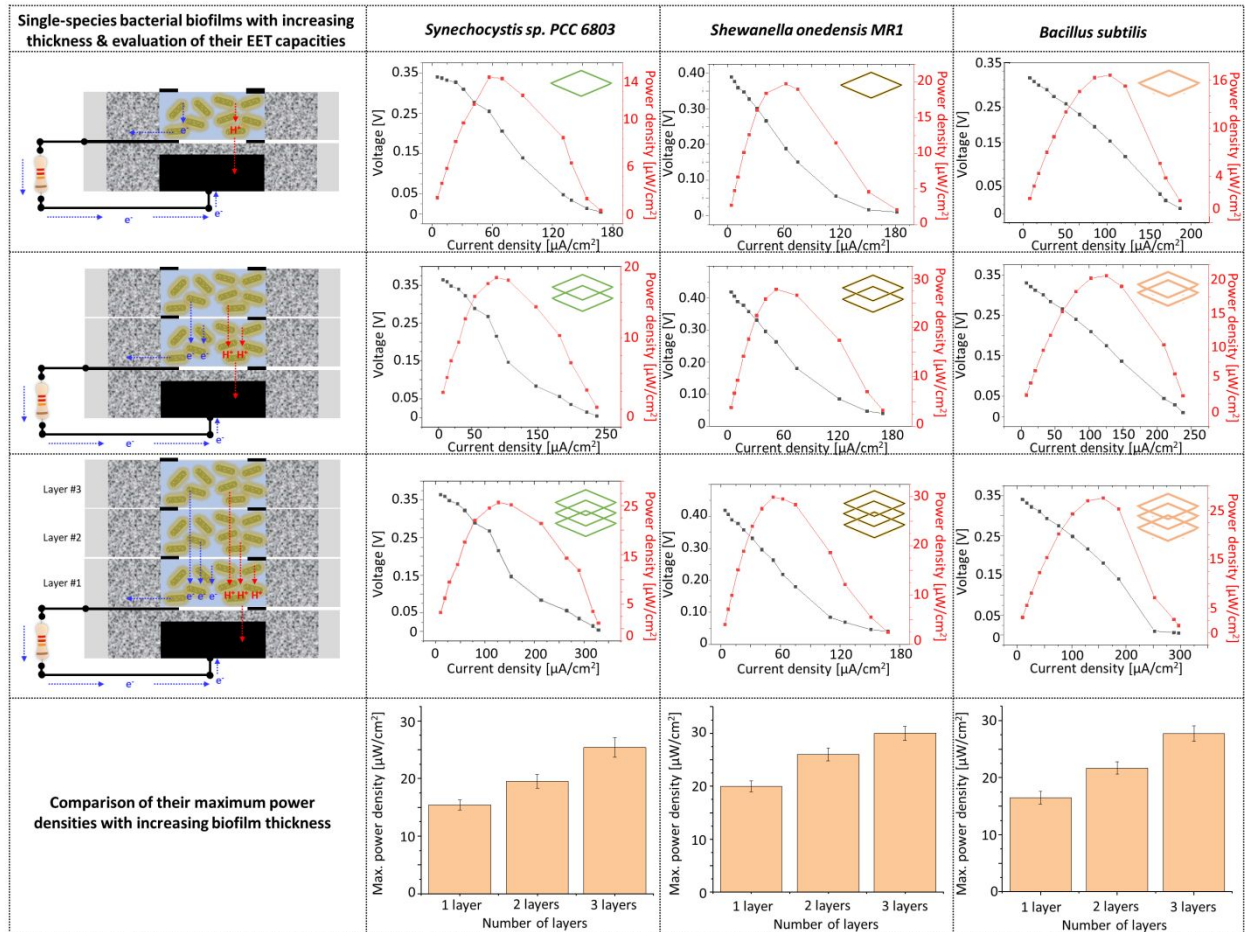


Figure 3. Evaluation of single-species bacterial EET capacities with increasing biofilm thickness. The schematic illustration of multi-laminar structures with patterned papers as a scaffold shows bacterial biofilm formation with different thickness. Three single-species, *Synechocystis sp. PCC6803*, *Shewanella oneidensis MR1*, and *Bacillus subtilis*, are tested. Polarization curves and output powers measured as a function of current are demonstrated. Finally, their maximum power densities with increasing biofilm thickness are compared.

1
2
3
4
5
6
7
8
9
10
11
12
13
14
15
16
17
18
19
20
21
22
23
24
25
26
27
28
29
30
31
32
33
34
35
36
37
38
39
40
41
42
43
44
45
46
47
48
49
50
51
52
53
54
55
56
57
58
59
60

Obviously, as the thickness of the biofilm increases, all three species have increased electrical performance. For a single layer, the best performance was clearly shown from *S. oneidensis* (*S. oneidensis*: 20 $\mu\text{W}/\text{cm}^2$, *Synechocystis sp.*: 15 $\mu\text{W}/\text{cm}^2$, and *B. subtilis*: 17 $\mu\text{W}/\text{cm}^2$). Even the other two generated comparable electrical outputs with increasing biofilm thickness (*S. oneidensis*: 30 $\mu\text{W}/\text{cm}^2$, *Synechocystis sp.*: 26 $\mu\text{W}/\text{cm}^2$, and *B. subtilis*: 28 $\mu\text{W}/\text{cm}^2$ for three layers). This is very surprising given that *Synechocystis sp.* and *B. subtilis* have weak electrogenic capabilities because of their low

1
2
3 1 EET efficiencies compared with *S. onedensis* having various EET mechanisms for much
4
5 2 greater electrogenic and electrochemical activities [3]. Thicker biofilms improve the EET
6
7 3 efficiencies of bacterial cells because of their increased numbers and the many conductive
8
9 4 conduits for electrons to move directly from the cells to the conductive fibers. Moreover,
10
11 5 when stacking the layers of the platform, the condition of the layer is impacted by
12
13 6 conductive conduits of the hosted species and the other EET mechanisms of the other
14
15 7 species surrounding it. Although further studies of chemical components of biofilms and
16
17 8 their conductivity are required, this result proves their better EET capabilities in biofilms,
18
19 9 providing one of the fundamental factors that can maximize bacterial electrochemical
20
21 10 performance.
22
23
24

25
26 11 Because the multi-layered paper system is patterned by hydrophobic wax boundaries and
27
28 12 its bottom cathodic layer is sealed, the system can only receive oxygen and nutrients through the
29
30 13 top window. (Figure 1 and Figure 3) [18, 19]. As nutrients and oxygen diffuse into the 3-D
31
32 14 biofilms from the top, the model provides decreasing gradients of nutrients and oxygen while the
33
34 15 simultaneous microbial metabolism increases gradients of waste products (e.g. protons, CO₂, etc.).
35
36 16 Our paper model can revolutionarily recapitulate the *in vivo* biofilm environment having
37
38 17 physiological stratification where each area is differently developed along those gradients.
39
40 18 Electrogenic bacterial cells on the top layer (#3) can rely more on oxygen for their respiration,
41
42 19 decreasing the electrode respiration and the current generation while the cells on the bottom layer
43
44 20 (#1) rather respire with the electrode and generate more electrons than the top layer. However,
45
46 21 the lack of nutrients on the bottom layer can negatively affect cell metabolism and viability.
47
48 22 When the cells oxidize the nutrients and produce electrons and protons in the multi-layered
49
50 23 system, the electrons move to the current collector on the top of the bottom layer and flow
51
52 24 through the external circuit to reach the cathode at the bottom of the bottom layer (Figure 3). In
53
54
55
56
57
58
59
60

1
2
3 1 the meantime, the protons diffuse to the bottom layer and travel to the cathode through the wax-
4
5 2 based separator. The Ag_2O is eventually reduced by the protons and electrons at the cathode to
6
7 3 maintain the charge neutrality of the MFC system. Because of the mass transfer limitation of the
8
9 4 protons, however, the protons can pile on the bottom layer decreasing pH and cell viability.
10
11 5 Understanding the microscale development of pH inside biofilms and its effect on cell viability
12
13 6 can allow for better-characterized correlations between bacterial EET activities in biofilm
14
15 7 thickness. MEMS microneedles were proposed as an alternative method for quantifying pH
16
17 8 inside biofilms, but their invasive technique uses ferricyanide, which kills the biofilm and thus
18
19 9 does not allow for time series measurements [29, 30]. The recently-developed pulsed-field
20
21 10 gradient Nuclear Magnetic Resonance (NMR) technique suffers from inherently low sensitivity
22
23 11 because of its low energies [30]. It requires careful optimization to reduce measurement times
24
25 12 and detect low concentrations. NMR systems are bulky, heavy, and expensive, further limiting
26
27 13 their capability and accessibility. Moreover, none of the techniques control biofilm thickness and
28
29 14 provide an effective analysis of cell viability across the biofilm thickness. De-stacking the multi-
30
31 15 layered biofilm construct can offer the most effective layer-by-layer analysis for pH distribution
32
33 16 and cellular viability at different biofilm locations. To determine the effect of the pH directly on
34
35 17 the cell viability after the MFC operation, we first avoided other potential factors to affect the cell
36
37 18 viability such as the nutrient and oxygen gradient. Before stacking the individual layers, they
38
39 19 were replenished with a fresh medium to eliminate a nutrient gradient. Furthermore, to avoid a
40
41 20 significant oxygen gradient, the biofilm construct was operated right after stacking. After 5 hours
42
43 21 of operation, we peeled apart the stacked layers and measured the pH and the cell viability of
44
45 22 each layer (Figure 4). The pH level was evaluated by using pH test strips and compared with the
46
47 23 initial culture pH (Figure 4a). For all bacterial species, a clear drop in pH was observed as each
48
49 24 layer got closer to the separator. Because other nutrient and gas gradients throughout the biofilm
50
51
52
53
54
55
56
57
58
59
60

1
2
3 1 were intentionally minimized, the increased acidification reduces cellular fitness and proliferation.
4
5
6
7
8
9
10
11
12
13
14
15
16
17
18
19
20
21
22
23
24
25
26
27
28
29
30
31
32
33
34
35
36
37
38
39
40
41
42
43
44
45
46
47
48
49
50
51
52
53
54
55
56
57
58
59
60

1
2
3
4
5
6
7
8
9
10
11
12
13
14
15
16
17
18
19
20
21
22
23
24
25
26
27
28
29
30
31
32
33
34
35
36
37
38
39
40
41
42
43
44
45
46
47
48
49
50
51
52
53
54
55
56
57
58
59
60

1 To better understand the change in bacteria viability caused by the decreased pH levels, the

1 bacterial cells were harvested from the individual layers, specifically containing *S. oneidensis*,
 2 and the dead/live cells were identified with fluorescent dyes with carboxyfluorescein diacetate
 3 (cFDA) and propidium iodide (PI) (Figure 4b). As the layers come closer to the separator and
 4 have lower pH, the fluorescent images indicate that the number of dead cells gradually
 5 outnumbers the live cells. The experiment demonstrates that there can be a steep decrease in
 6 local pH throughout biofilms during microbial metabolism, and the cell viability can be
 7 significantly reduced by the unequal pH distribution. This finding establishes fundamental
 8 knowledge to determine critical factors in improving bacterial EET activities within a thick
 9 biofilm.

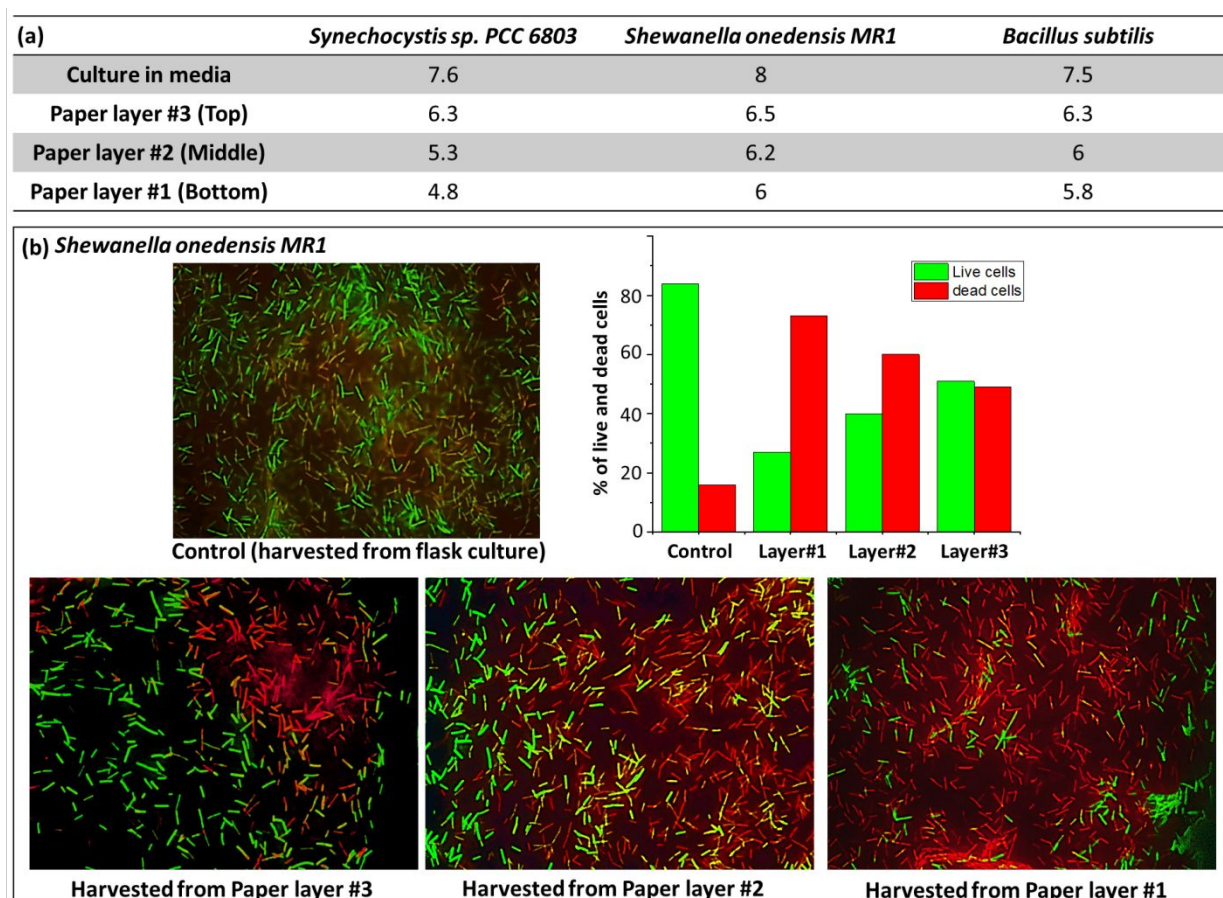


Figure 4. Layer-by-layer analysis after de-stacking three-layered biofilm constructs. (a) pH measurements of individual paper layers cultured with *Synechocystis sp.*, *Shewanella sp.*, and *Bacillus sp.*, respectively, compared with the values of species cultured in media. (b) Cell viability tests of individual three layers with *Shewanella sp.* Control is about the one harvested from flask media culture.

1
2
3 1
4
5 2 **2.2 Forming multilayered microbial consortium.** In the natural environment, bacteria
6
7
8 3 live in mixed communities having a complex heterogeneous environment with diverse
9
10 4 metabolic exchanges and co-dependencies [9-11]. Recent studies in multispecies
11
12 5 microbial consortia demonstrated their potential as an innovative approach enabling self-
13
14 6 sustainable, eco-friendly, and cost-effective biomanufacturing, biopowering, and
15
16 7 bioprocessing [12, 13, 31, 32]. On the other hand, many chronic infections require a better
17
18 8 understanding of such communities because they are related to polymicrobial biofilms
19
20 9 which are extremely difficult to be correctly diagnosed and effectively cured [33].
21
22 10 Therefore, the design and construction of artificial bacterial communities have opened a
23
24 11 new avenue in synthetic biology not only to develop new biofabrication technologies for
25
26 12 desired tasks but also to prevent and eradicate polymicrobial biofilms having detrimental
27
28 13 issues. However, multispecies biofilms are extremely difficult to model. Conventional
29
30 14 techniques are limited to uncontrollable and time-consuming mixed populations without
31
32 15 engineered *in vivo* stratification. Even the latest microfluidic approaches suffered from
33
34 16 very limited experimental setups with only a few selected strains. In that sense, our 3-D
35
36 17 multi-laminate paper stack can provide a new strategy for simple, rapid, and reliable
37
38 18 layer-by-layer polymicrobial biofilm formation in a controllable manner. Our paper-based
39
40 19 platform can potentially generate many different experimental setups to better understand
41
42 20 the individual and synergistic roles of key microbial populations. To quickly demonstrate
43
44 21 the potential and practicability of our technique for 3-D multispecies electroactive biofilm
45
46 22 engineering and compare its performance, we selected four two-species biofilms and two
47
48 23 three-species biofilms. In our previous study [12], we comprehensively explored
49
50 24 synergistic co-operations by using other biofabrication approaches having time-
51
52
53
54
55
56
57
58
59
60

1
2
3 1 consuming and complicated processes (Figure 5). Individual biofilm formation in paper
4
5 2 layers and multi-layered polymicrobial biofilm stacking followed the same procedure
6
7 3 described above but with different bacterial species. Our modular layer-by-layer platform
8
9 4 can design nature-like microscale spatial structures with different species while
10
11 5 maximizing their interaction and avoiding competition without physical contact between
12
13 6 species. While all individual bacterial biofilm layers showed a very similar range of
14
15 7 current generation as a result of collective EET activities in very conductive biofilms
16
17 8 (Figure 3), different combinations of bacterial species and their location generated
18
19 9 significantly different electrical performances (Figure 5). Under the illumination in a
20
21 10 fluorescent lamp-controlled chamber, the electrical performances of the two-species
22
23 11 biofilms were lower when *Synechocystis* sp. were located on the bottom than on the top
24
25 12 (Figure 5a). When the bacteria were in the bottom layer, light energy could not be fully
26
27 13 delivered to *Synechocystis* sp. through another species located on the top, and the EET
28
29 14 activities of *Synechocystis* sp. could not be added to the collective performance. Given
30
31 15 that *S. oneidensis* have a stronger electrogenic capability than *B. subtilis*, it is very
32
33 16 interesting that the combination with *S. oneidensis* (Figure 5a-1)) has a weaker electrical
34
35 17 performance than that with *B. subtilis* (Figure 5a-3)). Although the detailed chemical and
36
37 18 metabolic communications must be explored, it can be concluded that synergetic
38
39 19 cooperation can generate better and unexpected outputs. The three-species biofilm model
40
41 20 with *S. oneidensis* on the bottom produced the best performance among all multispecies
42
43 21 biofilms which is in good agreement with our previous study [12]. In this consortium, *B.*
44
45 22 *subtilis* located in the middle plays a critical role in improving the collective EET
46
47 23 activities. *B. subtilis* oxidize the organic compounds produced from *Synechocystis* sp.
48
49 24 located above and produce riboflavin as a product that can effectively mediate the EET
50
51
52
53
54
55
56
57
58
59
60

1
2
3 1 process of *S. oneidensis* on the bottom (Figure 5b-1)). When *B. subtilis* was located on the
4
5 2 bottom, the electrical performance dramatically decreased because the organic compounds
6
7 3 were not effectively delivered to the bottom (Figure 5b-1)). All the experiments were
8
9 4 conducted in triplicate, and data were represented as mean \pm standard deviation (Figure
10
11 5 S4). Although we have not provided additional data in this work, de-stacking the three-
12
13 6 layered biofilm construct will enable layer-by-layer analysis for further microbial and
14
15 7 genetic analyses. Our innovative modularity of the layer-by-layer construction of the
16
17 8 multi-species biofilm system can allow for emulating and elucidating those key
18
19 9 parameters and interactions between different biofilm layers, which have never been
20
21 10 explored in any previous studies.
22
23
24
25
26
27
28
29
30
31
32
33
34
35
36
37
38
39
40
41
42
43
44
45
46
47
48
49
50
51
52
53
54
55
56
57
58
59
60

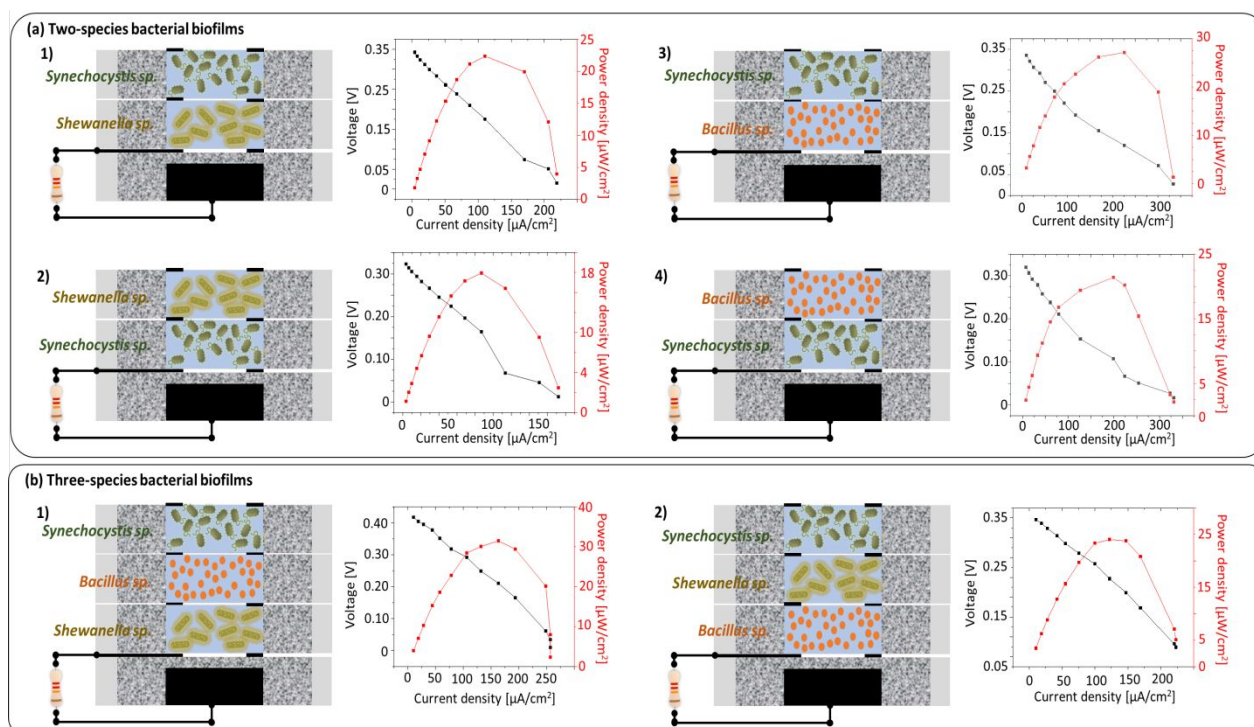


Figure 5. Evaluation of multiple-species bacterial EET capacities. (a) Schematic illustration of various two-species biofilms and their polarization/power curves (1. *Synechocystis sp.* (top) and *Shewanella sp.* (bottom); 2. *Shewanella sp.* (top) and *Synechocystis sp.* (bottom); 3. *Synechocystis sp.* (top) and *Bacillus sp.* (bottom); 4. *Bacillus sp.* (top) and *Synechocystis sp.* (bottom)). (b) Schematic illustration of two three-species biofilms and polarization/power curves (1. *Synechocystis sp.* (top), *Bacillus sp.* (middle), and *Shewanella sp.* (bottom); 2. *Synechocystis sp.* (top), *Shewanella sp.* (middle), and *Bacillus sp.* (bottom)).

3. Conclusion

In this work, we provided a new technique for biofabrication and characterization of a 3-D multi-species electroactive biofilm by using 3-D multi-laminate structures of papers as a scaffold. Multiple layers of paper containing individual bacterial cells were stacked to form a layered 3-D biofilm model that allowed us to control the thickness of the overall biofilm construct and the composition of each layer. Diffusions of the gas, nutrients, ions, and metabolites through the stack and the shapes of their gradients resemble the *in vivo* microenvironment of 3-D natural biofilms. By measuring the current generated from a

1 different number of layer stacks that integrated a MFC configuration, the overall EET
2 activities with different biofilm thicknesses were quantitatively characterized. De-stacking
3 the multi-layered biofilm construct allowed straightforward layer-by-layer analysis for pH
4 distribution and cellular viability. Multi-cultured stacks composed of paper layers formed
5 a multifunctional polymicrobial biofilm and increased the EET efficiency through
6 microbial syntrophic relationship. Overall electrogenic properties of different
7 combinations of bacterial cell types were readily investigated. The modularity of the
8 layer-by-layer construction of the culture system probed the complex interactions between
9 biofilm layers in the 3-D biofilm stack. Our paper-based platforms will revolutionize
10 characterizing and optimizing multi-species biofilm communities through the metabolic
11 engineering of organisms that can be incorporated into a practical bioelectrochemical
12 system.

14 **Materials and methods**

15 **Bacterial inoculum** All three bacterial species, *Synechocystis* sp. PCC 6803, *Shewanella*
16 *oneidensis* MR-1, and *Bacillus subtilis* were acquired from the American Type Culture
17 Collection (ATCC). *Synechocystis* sp. were grown at 30°C in a BG-11 medium in light
18 /dark cycles (12 hours/12 hours) for about two weeks. *S. oneidensis* were grown in an SB
19 medium with shaking for 24 hours at 30°C. *B. subtilis* were cultured overnight in an LB
20 medium at 37°C with shaking. Bacterial growth was monitored by using a
21 spectrophotometer with a wavelength of 600nm (OD₆₀₀) and all bacterial cultures were
22 used for tests when their OD₆₀₀ reached 1.0.

1 **Fabrication of layers of paper** Each layer of paper was prepared by directly patterning
2 wax onto Whatman Grade 1 filter paper sheets using a commercial wax printer
3 (ColorQube 8570). The wax-printed paper was placed in a 150°C oven for 60 seconds to
4 allow the impregnation of the wax through the entire thickness of the paper and to define
5 hydrophilic regions in the center with hydrophobic peripheral boundaries. The individual
6 papers were precisely cut by a laser cutter (Universal Laser System VLS 3.5) for further
7 biofilm formation and multi-laminate stacking. Conductive regions were prepared by
8 introducing a 20 μL mixture of 1 wt% PEDOT:PSS and 5 wt% dimethyl sulfoxide
9 (DMSO) into the hydrophilic areas. 20 μL of 2 wt% 3-glycidoxypropyl-trimethoxysilane
10 was added to the treated regions to improve their hydrophilicity and thus uniformly
11 distribute the liquid bacterial samples [28]. Circular graphite electrodes were then screen-
12 printed at the periphery of the conductive regions on both sides of the paper to act as the
13 current collector and the conductive interface when the individual papers are stacked. An
14 additional paper layer was prepared to integrate a wax-based separator and a cathode. The
15 penetration depth of the wax was carefully controlled so that the hydrophilic region was
16 secured from the back side of the paper sheet for the cathode. The cathode was prepared
17 by introducing 500 mg of silver (I) oxide (Ag_2O) in 10 mL PEDOT:PSS solution with 500
18 μL of DMSO. That layer was attached to the bacteria-containing layers to form an MFC
19 configuration. When the cells oxidize nutrients generating electrons and protons, the
20 electrons electrically move to the cathode through an external resistor and the protons
21 ionically flow to the cathode through the wax-based separator. Those collective electrons
22 are measured as a measure to determine the bacterial EET efficiencies.

23

1
2
3 1 **pH measurements and fluorescence imaging** To monitor the pH and the cell viability of
4
5 2 the individual paper layers, the layers of the stack were peeled apart. The pH level of each
6
7 3 layer was evaluated by pressing pH test strips on the layer and compared to the initial
8
9 4 culture pH. For the cell viability tests, the individual layers were submerged in phosphate-
10
11 5 buffered saline for the cells to be harvested through gentle sonication. The harvested cells
12
13 6 were double-stained with cFDA and PI, causing the live cells to fluoresce bright green and
14
15 7 dead cells to fluoresce red.
16
17
18
19 8

20
21 9 **SEM imaging** The SEM imaging protocol involved bacterial fixation in glutaraldehyde
22
23 10 2.5% in 0.1M PBS for 10 hours and dehydration steps in ascending ethanol series (35%,
24
25 11 50%, 75%, 95%, and 100%). The samples were further placed in a desiccator and left to
26
27 12 dry overnight. The samples were sputter-coated with carbon (208HR Turbo Sputter Coater,
28
29 13 Cressington Scientific Instruments, UK) and examined with a field emission SEM (Supra
30
31 14 55 VP, Carl Zeiss AG, German).
32
33
34
35
36
37
38
39
40
41
42
43
44
45
46
47
48
49
50
51
52
53

54 16 **Electrical measurement setup** The voltage drops across various external resistors (No
55
56 17 resistor, 470k, 250k, 162k, 100k, 71k, 47.5k, 32k, 22k, 15k, 10k, 2k, 1.5k, 0.45k, and
57
58 18 0.35k) were monitored with a data acquisition system (National Instruments, USB-6212).
59
60 19 The power outputs and polarization curves were acquired through calculation with the
61
62 20 voltage values at those resistors. Power and current densities were normalized to the
63
64 21 anode surface area.
65
66
67
68
69
70

71 23 **Author contributions**

1 Anwar Elhadad: Investigation; Methodology; Formal analysis; Data curation; Validation;
2
3
4
5 2 Software
6
7
8 3 Seokheun Choi: Conceptualization; Supervision; Project administration; Funding acquisition;
9
10 4 Writing – original draft; Writing – review, editing, and finalization.
11
12
13 5
14

15 6 **Conflicts of interest**

16
17 7 There are no conflicts to declare.
18
19
20 8
21

22 9 **Acknowledgments**

23
24
25 10 This work was supported mainly by the National Science Foundation (CBET #2100757) and the
26
27 11 Office of Naval Research (#N00014-21-1-2412), and partially by the National Science
28
29 12 Foundation (ECCS #2020486, and ECCS #1920979).
30
31
32 13
33

34 14 **References**

- 35
36
37 15 1. J. Zhao, F. Li, Y. Cao, X. Zhang, T. Chen, H. Song, Z. Wang, “Microbial extracellular
38 16 electron transfer and strategies for engineering electroactive microorganisms,” *Biotechnology*
39 17 *Advances*, 53, 107682, 2021.
- 40
41 18 2. Y. Jiang, R.J. Zeng, “Bidirectional extracellular electron transfers of electrode-biofilm:
42 19 Mechanism and application,” *Bioresource Technology*, 271, 439, 2019.
- 43
44 20 3. B.E. Logan, R. Rossi, A. Ragab, P.E. Saikaly, “Electroactive microorganisms in
45 21 bioelectrochemical systems,” *Nature Reviews Microbiology*, 17, 307, 2019.
- 46
47 22 4. D.R. Lovley, “Electromicrobiology,” *Annual Review of Microbiology*, 66, 391, 2012.
- 48
49 23 5. C. Tseng, J.J. Silberg, G.N. Bennett, R. Verduzco, “100th anniversary of macromolecular
50 24 science viewpoint: soft materials for microbial bioelectronics,” *ACS Macro Letters*, 9, 1590,
51 25 2020.
52
53
54
55
56
57
58
59
60

- 1
2
3 1 6. S. Choi, "Electrogenic Bacteria Promise New Opportunities for Powering, Sensing, and
4 2 Synthesizing," *Small*, 2107902, 2022.
- 5
6 3 7. A. Prominski, B. Tian, "Bridging the gap – biomimetic design of bioelectronic interfaces,"
7 4 *Current Opinion in Biotechnology*, 72, 69, 2021.
- 8
9 5 8. M.T. Mee, J.J. Collins, G.M. Church, H.H. Wang, "Syntrophic exchange in synthetic
10 6 microbial communities," *PNAS*, E2149-E2156, 2014.
- 11
12 7 9. C.M. Agapakis, P.M. Boyle, P.A. Silver, "Natural strategies for the spatial optimization of
13 8 metabolism in synthetic biology," *Nature Chemical Biology*, 8, 527, 2012.
- 14
15 9 10. H. Wu, C. Moser, H. Wang, N. Hoiby, Z. Song, "Strategies for combating bacterial biofilm
16 10 infections," *International Journal of Oral Science*, 7, 1, 2015.
- 17
18 11 11. H.J. Kim, J.Q. Boedicker, J.W. Choi, R.F. Ismagilov, "Defined spatial structure stabilizes a
19 12 synthetic multispecies bacterial community," *PNAS*, 105, 18188, 2008.
- 20
21 13 12. L., Liu, M. Mohammadifar, A. Elhadad, M. Tahernia, Y. Zhang, W. Zhao, and S. Choi,
22 14 "SPATIAL ENGINEERING OF MICROBIAL CONSORTIUM for Long-lasting, Self-
23 15 sustaining, and High-power Generation in a Bacteria-powered Biobattery," *Advanced Energy*
24 16 *Materials*, 11, 2100713, 2021.
- 25
26 17 13. Y. Liu, M. Ding, W. Ling, Y. Yang, X. Zhou, B. Li, T. Chen, Y. Nie, M. Wang, B. Zeng, X.
27 18 Li, H. Liu, B. Sun, H. Xu, J. Zhang, Y. Jiao, Y. Hou, H. Yang, S. Xiao, Q. Liu, X. He, W.
28 19 Liao, Z. Jin, Y. Xie, B. Zhang, T. Li, X. Lu, J. Li, F. Zhang, X. Wu, H. Song, Y. Yuan, "A
29 20 three-species microbial consortium for power generation," *Energy & Environmental Science*,
30 21 10, 1600, 2017.
- 31
32 22 14. R.L. Shahab, S. Brethauer, M.P. Davey, A.G. Smith, S. Vignolini, J.S. Luterbacher, M.H.
33 23 Studer, "A heterogeneous microbial consortium producing short-chain fatty acids from
34 24 lignocellulose," *Science*, 369, 1073, 2020.
- 35
36 25 15. L.J. Bird, E.L. Onderko, D.A. Phillips, R.L. Mickol, A.P. Malanoski, M.D. Yates, B.J. Eddie,
37 26 S.M. Glaven, "Engineered living conductive biofilms as functional materials," *MRS*
38 27 *Communications*, 9, 505, 2019.
- 39
40 28 16. H. Beyenal, J.T. Babauta, "Microscale gradients and their role in electron-transfer
41 29 mechanisms in biofilms," *Biochem. Soc. Trans.*, 40, 1315, 2012.
- 42
43 30 17. G. Choi, and S. Choi, "Monitoring electron and proton diffusion flux through three-
44 31 dimensional, paper-based, variable biofilm and liquid media layers," *Analyst*, 140, 5901,
45 32 2015.
- 46
47 33 18. D. Lantigua, Y. N. Kelly, B. Unal, G. Camci-Unal, "Engineered paper-based cell culture
48 34 platforms," *Advanced Healthcare Materials*, 6, 1700619, 2017.

19. B. Mosadegh, B.E. Dabiri, M.R. Lockett, R. Derda, P. Campbell, K.K. Parker, G.M. Whitesides, "Three-dimensional paper-based model for cardiac ischemia," *Advanced Healthcare Materials*, 3, 1036, 2014.
20. T. Agarwal, M.R. Borrelli, P. Makvandi, M. Ashrafizadeh, T.K. Maiti, "Paper-based cell culture: paving the pathway for liver tissue model development on a cellulose paper chip," *ACS Applied Bio Materials*, 3, 2956, 2020.
21. A.P. Borole, G. Reguera, B. Ringeisen, Z. Wang, Y. Feng, B.H. Kim, "Electroactive biofilms: Current status and future research needs," *Energy & Environmental Science*, 4, 4813, 2011.
22. D. Davila, J. P. Esquivel, N. Sabate, J. Mas, "Silicon-based microfabricated microbial fuel cell toxicity sensor," *Biosensors and Bioelectronics*, 26, 2426, 2011.
23. M.J. Franklin, C. Chang, T. Akiyama, B. Bothner, "New Technologies for Studying Biofilms," *Microbiology Spectrum*, 3, 10.1128, 2016.
24. R.N. Alnahhas, J.J. Winkle, A.J. Hirning, B. Karamched, W. Ott, K. Josic, M.R. Bennett, "Spatiotemporal dynamics of synthetic microbial consortia in microfluidic devices," *ACS Synthetic Biology*, 8, 2051, 2019.
25. V. Kantsler, E. Ontanon-McDonald, C. Kuey, M.J. Ghanshyam, M.C. Roffin, M. Asally, "Pattern Engineering of Living Bacterial Colonies Using Meniscus-Driven Fluidic Channels," *ACS Synthetic Biology*, 9, 1277, 2020.
26. S. Balasubramanian, K. Yu, D.V. Cardenas, M. Aubin-Tam, A.S. Meyer, "Emergent biological endurance depends on extracellular matrix composition of three-dimensionally printed *Escherichia coli* biofilms," *ACS Synthetic Biology*, 9, 2997, 2021.
27. E. Ning, G. Turnbull, J. Clarke, F. Picard, P. Riches, M. Vendrell, D. Graham, A.W. Wark, K. Faulds, W. Shu, "3D bioprinting of mature bacterial biofilms for antimicrobial resistance drug testing," *Biofabrication*, 11, 045018, 2019.
28. Y. Gao and S. Choi, "Merging Electric Bacteria with Paper," *Advanced Materials Technologies*, 3, 1800118, 2018.
29. H. Lee, W. Choi, X. Guo, W.R. Heineman, P.L. Bishop, "Material science chemistry of electrochemical microsensors and applications for biofilm research," *Key Engineering Materials*, 521, 113, 2012.
30. R.S. Renslow, J.T. Babauta, P.D. Majors, H. Beyenal, "Diffusion in biofilms respiring on electrodes," *Energy & Environmental Science*, 6, 595, 2013.
31. K. Brenner, L. You, F.H. Arnold, "Engineering microbial consortia: a new frontier in synthetic biology," *Trends in Biotechnology*, 26, 483, 2008.

1
2
3
4
5
6
7
8
9
10
11
12
13
14
15
16
17
18
19
20
21
22
23
24
25
26
27
28
29
30
31
32
33
34
35
36
37
38
39
40
41
42
43
44
45
46
47
48
49
50
51
52
53
54
55
56
57
58
59
60

1 32. D.J. Kenny, E.P. Balskus, "Engineering chemical interactions in microbial communities,"
2 Chem. Soc. Rev. 47, 1705, 2018.

3 33. H.M.E. Willems, Z. Xu, B.M. Peters, "Polymicrobial biofilm studies: from basic science to
4 biofilm control," Curr. Oral Health Rep., 3, 36, 2016.